JOURNAL OF COMPUTATIONAL PHYSICS 97, 73–90 (1991)

Exact Analysis of Nonlinear Instability in a Discrete Burgers' Equation

M. F. MARITZ AND S. W. SCHOOMBIE

Department of Applied Mathematics,
University of the Orange Free State, Bloemfontein 9300, South Africa

Received September 26, 1989; revised August 22, 1990

A family of explicit nonlinear numerical schemes for Burgers' equation is derived by means of a discrete version of the Hopf–Cole transformation. Exact nonlinear stability conditions for these schemes are then found, and for one particular scheme the exact stability criteria are compared to the conventional linearized stability condition.

1. INTRODUCTION

The stability criteria of *linear* evolution difference equations with periodic boundary conditions are easily found by applying a standard von Neumann analysis and the mechanism for linear blowup (exponentially growing modes) is fully understood. Even when nonperiodic boundary conditions are imposed and equations with variable coefficients are considered [1–5], probing the mechanisms which cause instability is relatively easy compared to understanding the causes of instability in fully nonlinear equations, where little is known. In our view it would be of considerable instructive value to have a nonlinear difference equation available of which the exact solution can be found *and* which displays typical nonlinear blowup. The analysis of such a blowup phenomenon (which would in principle be possible, because the exact solution can be found) might reveal much about the origin of and mechanism causing nonlinear blowup in nonlinear partial difference schemes. This is exactly what we intend to do in this paper.

Using a discrete Hopf–Cole transformation (HCT), we derive a family of explicit nonlinear difference schemes for Burgers' equation

$$u_t - 2\alpha\sigma u u_x - \sigma u_{xx} = 0, \qquad \sigma > 0, \tag{1}$$

of which the exact stability criteria are known and of which the nonlinear blowup mechanism is well understood.

In contrast to linear blowup, which is global, exponentially growing and (with periodic boundary conditions) independent of the initial condition, numerical experimental experience indicates that the blowup in nonlinear schemes are often

0021-9991/91 $3.00

— local [6],

— very sudden rather than exponentially growing [6–8] (the solution seems to encounter a singularity in time),

— dependent on the initial condition [6, 8, 11] (even with periodic boundary conditions).

The family of schemes that we derive here display all these characteristics, but the important point is that we can, in this particular case, understand why and how it happens. These schemes also display a typical linear blowup, when an associated linear stability condition is violated, and hence demonstrates that the same nonlinear scheme can display various kinds of instabilities.

We wish to stress that these schemes are special, and it is highly unlikely that other nonlinear schemes would lend themselves to precisely such an analysis, but we feel that the knowledge gained by studying these special schemes might give new insight into the nature of nonlinear instabilities. Techniques such as linearizing (see, e.g., [12]), discrete multiple scales analysis [13, 14], and other perturbational techniques are essentially concerned with weak nonlinearities, while studying an associated system of nonlinear ODEs [9–11] or studying the interaction of a small number of modes [6, 15, 16], could limit the scope for which the analysis is appropriate. We consider here fully discretized, fully nonlinear schemes and assume that the solution may contain any number of modes or be represented by any number of points in space. Since the exact nonlinear stability criteria of these schemes are known, we also want to propose these schemes as prototype examples on which many of the above-mentioned techniques can be tried.

2. Remarks on the Continuous Hopf–Cole Transformation

The continuous Hopf–Cole transformation, first introduced by Hopf [17] in 1950 and independently by Cole [18] in 1951, is a member of the Bäcklund transformations which are sets of equations relating solutions of one partial differential equation to those of another. The relevant differential equations are usually nonlinear, but in the case of the Hopf–Cole transformation one is the linear heat equation

$$v_t - \sigma v_{xx} = 0. \tag{2}$$

The solutions of Eq. (1) are mapped to solutions of Eq. (2) by the Hopf–Cole transformation

$$u = \frac{v_x}{\alpha v}. \tag{3}$$

Since solutions of the Heat equation are obtainable by means of the Fourier transform or other integral transforms, solutions of Burgers' equation can be obtained

via this mapping. For integral representations of exact solutions of Burgers' equation see Whitham [19, Chap. 4].

This method of obtaining solutions to nonlinear PDEs via linearizing transformations have been generalized and extended by, among others, Sachdev [20] and Tasso and Teichmann [21]. The generalizations involved consist of considering other linear PDEs than the heat equation and mapping them via the Hopf–Cole transformation to nonlinear PDEs. Time and space dependent coefficients are introduced, and systems of coupled equations are also considered. In [22] matrix versions of Burgers' equation are considered and a semidiscretization of these matrix Burgers' systems is presented. In [23] fully discrete nonlinear difference equations are derived for the scalar case with general Hopf–Cole transformations containing higher order differences.

In the following section we shall introduce a fully discrete Hopf–Cole transformation which maps discrete versions of the linear heat equation to discrete versions of Burgers' equation.

3. Derivation of the Nonlinear Schemes

We shall first show how a general linear evolution difference equation with Euler time-stepping is transformed into a nonlinear difference equation also with a disguised form of Euler time-stepping by means of a discrete analogue of the Hopf–Cole transformation.

We discretize the space variable as

$$x = hj, \qquad j \in \mathbb{Z},$$

and the time variable as

$$t = kn, \qquad n = 0, 1, ...,$$

and use the following approximations for the continuous functions v and u:

$$V_j^n \approx v(hj, kn),$$
$$U_j^n \approx u(hj, kn).$$

In order to save space in some of the lengthy formulae in this section and to increase readability, we shall present all formulae in this section just for the node with $n = 0$ and $j = 0$. Then, whenever a superscript is zero, we shall simply suppress it. Thus a formula of the form $f(V_j^{n+1}, V_j^n, V_{j+1}^n, V_{j-1}^n)$ will be written as $f(V_0^1, V_0, V_1, V_{-1})$.

We also introduce the *factorial power* [24] of a discrete function A_j as

$$A_j^{(m)} = \prod_{i=j}^{m+j-1} A_i,$$

and the inverse factorial power

$$A_j^{(-m)} = \prod_{i=j+1}^{m+j} \frac{1}{A_{-i}}, \qquad A_j^{(0)} = 1.$$

Throughout this paper the factorial notation will only apply to subscripts.

The continuous HCT can be expressed in the following convenient format

$$v_x = \alpha uv, \tag{4}$$

where α is a constant.

We now discretize (4) using a forward difference approximation for v_x and a weighted average for v:

$$\frac{V_1 - V_0}{h} = \frac{1}{2}\alpha U_0[(1+\theta)V_0 + (1-\theta)V_1] \tag{5}$$

which can be expressed as

$$V_1 = f_0 \cdot V_0, \tag{6}$$

where

$$f_0 = \frac{1 + \alpha h(1+\theta)U_0/2}{1 - \alpha h(1-\theta)U_0/2}. \tag{7}$$

and $\theta \in [-1, 1]$.

Applying (6) recursively and using the factorial power notation, we can write

$$V_j = f_0^{(j)} \cdot V_0. \tag{8}$$

We now consider a general discrete linear evolution equation of the form

$$V_0^1 = \sum_{j=J_0}^{J_0+J} b_j V_j, \tag{9}$$

where the b_j are constants.

By substituting (8) into (9), we obtain

$$V_0^1 = \left(\sum_{j=J_0}^{J_0+J} b_j f_0^{(j)}\right) \cdot V_0. \tag{10}$$

We now obtain V_1^1 in two ways—by shifting (6) in time and shifting (10) in space:

$$V_1^1 = f_0^1 V_0^1 = f_0^1 \left(\sum_{j=J_0}^{J_0+J} b_j f_0^{(j)}\right) \cdot V_0$$

$$V_1^1 = f_0 \left(\sum_{j=J_0}^{J_0+J} b_j f_1^{(j)}\right) \cdot V_0.$$

Assuming that $V_0 \not\equiv 0$, elimination of V_1^1 and V_0 from both these equations gives

$$f_0^1\left(\sum_{j=J_0}^{J_0+J} b_j f_0^{(j)}\right) = f_0\left(\sum_{j=J_0}^{J_0+J} b_j f_1^{(j)}\right)$$

which can also be expressed as

$$(f_0^1 - f_0)\sum_{j=J_0}^{J_0+J} b_j f_0^{(j)} = f_0 \sum_{j=J_0}^{J_0+J} b_j (f_1^{(j)} - f_0^{(j)}), \tag{11}$$

where the Euler time-stepping approximation on the left-hand side is more evident.

We now consider a discrete heat equation of the form

$$\left(\frac{V_0^1 - V_0}{k}\right) = \sigma\left(\frac{V_1 - 2V_0 + V_{-1}}{h^2}\right) \tag{12}$$

with σ the positive diffusivity constant. Rewrite (12) as

$$V_0^1 = b_{-1}V_{-1} + b_0 V_0 + b_1 V_1, \tag{13}$$

where

$$b_{-1} = b_1 = r, \qquad b_0 = 1 - 2r, \qquad \text{with} \quad r = k\sigma/h^2.$$

Using the discrete Hopf–Cole transformation (6), with f_0 given by (7), evaluation of (11) gives the following discretization of Burgers' equation:

$$\begin{aligned}
&(U_0^1 - U_0)[1 - \tfrac{1}{2}\alpha hr\theta(U_1 - 2U_0 + U_{-1}) + \tfrac{1}{2}\alpha h(r-1)(U_1 - U_{-1}) \\
&\quad + \tfrac{1}{2}\alpha h\theta(U_1 + U_{-1}) - \tfrac{1}{2}\alpha^2 h^2 r\theta U_0(U_1 - U_{-1}) \\
&\quad + \tfrac{1}{4}\alpha^2 h^2 r(\theta^2 + 1)(U_0 U_1 - 2U_1 U_{-1} + U_0 U_{-1}) + \tfrac{1}{4}\alpha^2 h^2(\theta^2 - 1)\, U_1 U_{-1}] \\
&= r(U_1 - 2U_0 + U_{-1}) + \alpha hr[U_0(U_1 - U_{-1}) + \theta(U_1 U_{-1} - (U_0)^2)] \\
&\quad + \tfrac{1}{2}\alpha^2 h^2 r\theta(U_0)^2(U_1 - U_{-1}) \\
&\quad - \tfrac{1}{4}\alpha^2 h^2 r(1 + \theta^2)\, U_0(U_1 U_0 - 2U_1 U_{-1} + U_0 U_{-1}).
\end{aligned} \tag{14}$$

We shall refer to this scheme as the *general* discrete Burgers' equation.

For our subsequent discussion, we shall only use two special cases of this general formula: $\theta = 1$, which we shall call the *skew* scheme and will be used in the discussion of the boundary conditions in Section 4; and $\theta = 0$ which we shall call the *central* scheme for which we shall do a linearized stability analysis in Section 6, and which will be used mostly in the numerical experiments in Section 7.

The central scheme ($\theta = 0$) is given by

$$\left(\frac{U_0^1 - U_0}{k}\right)\left[1 + \alpha(k\sigma - h^2)\left(\frac{U_1 - U_{-1}}{2h}\right)\right.$$
$$\left. - \frac{\alpha^2 h^2}{4} U_1 U_{-1} + \frac{k\sigma\alpha^2}{4}(U_0 U_{-1} + 2U_1 U_{-1} + U_0 U_1)\right]$$
$$= \sigma\left(\frac{U_1 - 2U_0 + U_{-1}}{h^2}\right) + 2\sigma\alpha U_0\left(\frac{U_1 - U_{-1}}{2h}\right)$$
$$- \frac{\sigma\alpha^2}{4} U_0(U_1 U_0 - 2U_1 U_{-1} + U_0 U_{-1}) \tag{15}$$

which approximates Burgers' equation to the *second* order in h and first order in k:

$$u_t[1 + (O(k) + O(h^2))(u_x + u^2)] = \sigma u_{xx} + 2\alpha\sigma u u_x + O(h^2)\, u(2u_x^2 - u u_{xx}). \tag{16}$$

The skew scheme ($\theta = 1$) is given by

$$\left(\frac{U_0^1 - U_0}{k}\right)\left[1 + \alpha h U_{-1} + \alpha\sigma k\left(\frac{U_0 - U_{-1}}{h}\right) + \alpha^2\sigma k U_0 U_{-1}\right]$$
$$= \sigma\left(\frac{U_1 - 2U_0 + U_{-1}}{h^2}\right) + 2\alpha\sigma\left(\frac{U_0 + U_{-1}}{2}\right)\left(\frac{U_1 - U_0}{h}\right)$$
$$+ \alpha^2\sigma h U_0 U_{-1}\left(\frac{U_1 - U_0}{h}\right). \tag{17}$$

This scheme approximates Burgers' equation to first order in both h and k:

$$u_t[1 + O(h)u + O(k)u_x + O(k)u^2] = \sigma u_{xx} + 2\alpha\sigma u u_z + O(h)\, u^2 u_x. \tag{18}$$

4. Treatment of Initial and Boundary Conditions

Since the treatment of the special boundary conditions for V_j^n is substantially easier if one has a non-rational form for f_j^n, we discuss only the case of the skew scheme ($\theta = 1$), for which

$$f_j^n = 1 + \alpha h U_j^n.$$

The general case is similar, but the manipulations are more involved.

Continuous Case

Assume that Burgers' equation

$$u_t - 2\alpha\sigma u_x - \sigma u_{xx} = 0$$

is to be solved with periodic boundary conditions,

$$u(x, t) = u(x + b, t), \qquad \text{for all} \quad x \in \mathbb{R}, t \geqslant 0,$$

and with a b-periodic initial condition,

$$u(x, 0) = u(x + b, 0), \qquad x \in \mathbb{R}.$$

Using the HCT, (4), it is easy to show that

$$v(x + b, t) = v(x, t) \exp(\alpha C(t)),$$

where

$$C(t) = \int_x^{x+b} u(\xi, t)\, d\xi,$$

but since $u(x, t)$ is b-periodic in space and satisfies Burgers' equation (1), $dC(t)/dt = 0$; hence $C(t)$ is constant. The problem can thus be solved by transforming the periodic initial condition for u over one period to the initial condition for v using the HCT and choosing (arbitrarily) $v(0, 0) = 1$. The heat equation is then solved using this initial condition with the following boundary conditions:

$$v(x + b, t) = v(x, t) \exp(\alpha C(0)).$$

Discrete Case

For the discrete case, let $h = b/N$ and $U_j^0 = u(hj, 0)$, $j = 0, 1, ..., N-1$. For periodic U_j^n, the appropriate periodic boundary conditions are

$$U_j^n = U_{j+N}^n. \tag{19}$$

Applying the discrete HCT,

$$V_{j+1}^n = (1 + \alpha h U_j^n)\, V_j^n; \tag{20}$$

recursively, it can be shown that V_j^n satisfies

$$V_{kN+j}^n = V_j^n (C_n)^k \qquad \text{for} \quad j = 0, 1, ..., N-1 \text{ and } k \in \mathbb{Z}, \tag{21}$$

where

$$C_n = (1 + \alpha h U_j^n)^{(N)}. \tag{22}$$

We now proceed to prove that C_n is independent of n. Stating that U_j^n satisfies the discrete Burgers' equation (17) is equivalent to stating that V_j^n satisfies the discrete heat equation (12) *and* that the discrete HCT (20) applies. In order to

avoid complicated manipulations we shall never use (17) directly, but make use of the above argument.

Using (20) and the discrete heat equation (12) it can be shown that

$$V_j^{n+1} = \left[1 + r\left(-1 + \alpha h U_j^n + \frac{1}{1 + \alpha h U_{j-1}^n}\right)\right] V_j^n. \tag{23}$$

Now from (21) it follows that

$$C_{n+1} = \frac{V_{j+N}^{n+1}}{V_j^{n+1}} \quad \text{and} \quad C_n = \frac{V_{j+N}^n}{V_j^n}.$$

Using the relationship (23), one finds

$$C_{n+1} = \frac{[1 + r(-1 + \alpha h U_{j+N}^n + 1/(1 + \alpha h U_{j+N-1}^n))]\, V_{j+N}^n}{[1 + r(-1 + \alpha h U_j^n + 1/(1 + \alpha h U_{j-1}^n))]\, V_j^n}$$

and, imposing the periodic boundary conditions for U_j^n, (19), it follows that

$$C_{n+1} = \frac{V_{j+N}^n}{V_j^n} = C_n.$$

The appropriate boundary conditions for V_j^n are then

$$V_{j+N}^n = V_j^n C_0, \tag{24}$$

and one can arbitrarily choose $V_0^0 = 1$. Thus the discrete heat equation (12) can be solved over a single period with the boundary conditions

$$V_N^n = C_0 V_0^n, \qquad V_{-1}^n = V_{N-1}^n / C_0,$$

and on any chosen time level the solution V_j^n can be transformed into the corresponding solution for U_j^n. However, we do not intend to solve Burgers' equation this way, but we merely want to derive from this how the nonlinear scheme for Burgers' equation can become unstable.

5. Exact Stability Criteria

The key to understanding the stability properties of the general discrete Burgers' equation (14), lies in the relationship between V_j^n and U_j^n, which is the discrete HCT,

$$U_j^n = \frac{2(V_{j+1}^n - V_j^n)}{\alpha h((1-\theta)\, V_{j+1}^n + (1+\theta)\, V_j^n)}. \tag{25}$$

Two kinds of unphysical behavior can occur in the solution U_j^n:

(a) V_j^n may be linearly unstable (due to its linear stability condition being violated) and will display growing high frequency modes, and this will naturally be transferred to the behavior of U_j^n which then is the quotient of two oscillating functions.

(b) the denominator in (25) may beome zero, which will cause U_j^n to display a singularity.

The condition mentioned in (a) is imply the von Neumann stability condition for the discrete Heat equation, (12), and is given by [25]

$$r \leqslant \frac{1}{2} \qquad \left(\text{that is, } k \leqslant \frac{h^2}{2\sigma}\right). \tag{26}$$

We shall refer to this condition as the *linear stability condition.*

Turning to the condition mentioned in (b): Under what conditions will the denominator in (25) become zero? (In a computer implementation, it only has to become small enough to cause an overflow.) For the case $\theta = \pm 1$, it is clear that V_j^n must become zero for some j and n, in order to cause U_j^n to display singular behavior. For $\theta \neq \pm 1$, V_j^n must differ in sign on two consecutive nodes for the denominator to vanish. Thus positivity of V_j^n (for all n and j) is a sufficient condition to guarantee that U_j^n will not display singular behavior.

It should be noted that the linear stability condition $0 < r < \frac{1}{2}$ also guarantees that $b_{-1} > 0$, $b_0 > 0$, and $b_1 > 0$ in formula (13). So if initially V_j^0 is positive for all j, any subsequent V_j^n will never become negative. Thus satisfying the von Neumann stability condition also guarantees that U_j^n will display no singular behavior as long as V_j^0 is positive throughout.

However, if initially V_j^0 has both positive and negative parts (since it is a discrete function, it need not have any zeros), it may develop a condition where the denominator in (25) vanishes, as it evolves according to the discrete heat equation.

Now from (6) V_j^0 is calculated as

$$V_j^0 = (f_0^0)^{(j)} V_0^0. \tag{27}$$

If we choose $V_0^0 = 1$, positivity of V_j^0 is guaranteed, when none of the factors in the product $(f_0^0)^{(j)}$ in (27) are negative, i.e., when

$$f_j^0 \geqslant 0 \qquad \text{for all} \quad j = 0, 1, \ldots, N-1. \tag{28}$$

Since U_j^0 appears in the expression for f_j^0, it means that the initial condition, U_j^0, is also significant in determining the stability of the scheme.

We shall refer to condition (28) which renders V_j^0 positive throughout as the *nonlinear stability condition.*

For the general scheme (14), a necessary and sufficient nonlinear condition for (28) to hold is

$$\frac{-2}{\alpha h(1+\theta)} < U_j^0 < \frac{2}{\alpha h(1-\theta)} \qquad \text{for all } j \tag{29}$$

when $\alpha > 0$, and when $\alpha < 0$, the directions of the inequalities are reversed.

For the rest of this paper, let $U_{\max} = \max_j |U_j^0|$.

For the skew scheme ($\theta = 1$), the nonlinear stability condition can be expressed as

$$h \leqslant \frac{-1}{\alpha U_{\max}} \tag{30}$$

for negative α, and we have unconditional nonlinear stability for positive α. Thus if $\alpha > 0$ and the linear stability condition is satisfied, we have a scheme for Burgers' equation which is stable for all h and $U_{\max}$! This fact will be explored in the first numerical experiment in Section 7.

For the central scheme ($\theta = 0$), the nonlinear stability condition is

$$|\alpha h U_{\max}| < 2. \tag{31}$$

Henceforth we shall refer to the linear and nonlinear stability conditions jointly as the *exact* stability conditions.

5. The Linearized Stability Condition

To what extent can a von Neumann analysis of the associated linearized scheme predict the stability of a nonlinear scheme? It is well known that linearization gives a fairly accurate stability condition as long as the ansatz for linearization, namely that the solution is a small perturbation about a constant is satisfied. For solutions away from these, linearization cannot be trusted, in general.

We shall now do a von Neumann analysis of a linearized version of the central scheme, (15), and compare the results with the exact stability conditions available. The results are interesting: there is a close correspondence between the two sets of conditions, but linearization predicts stability in a region where the scheme is definitely unstable according to the exact stability conditions.

Set $U_j^n = \bar{U} + \varepsilon W_j^n$, and assuming that ε is small, we neglect all quadratic and higher order terms in ε. The perturbation, W_j^n, then satisfies the difference equation

$$W_j^{n+1} - W_j^n = A(W_{j+1}^n - 2W_j^n + W_{j-1}^n) + B(W_{j+1}^n - W_{j-1}^n), \tag{32}$$

where

$$A = \frac{r(4+P^2)}{4+P^2(4r-1)}, \qquad B = \frac{4rp}{4+P^2(4r-1)}, \qquad P = \alpha h \bar{U}.$$

Note that $|A| \geqslant |B|$ for all $r > 0$ and any real P, and also that for all $r > 0$, $A \neq 0$.

The discrete dispersion relation for a single mode of the form

$$W_j^n = \xi^n e^{i\kappa j}$$

is given by

$$\xi = 1 + 2A(\cos\kappa - 1) + 2iB\sin\kappa \tag{33}$$

and requiring no growth for this mode imposes the condition

$$(1-\cos\kappa)[(A^2 - B^2)\cos\kappa + (A - A^2 - B^2)] \geqslant 0. \tag{34}$$

For all $\kappa \in [0, \pi]$, (34) will be satisfied if and only if

$$A \geqslant 2A^2 \tag{35}$$

and

$$A \geqslant B^2. \tag{36}$$

These conditions rule out the possibility of A being negative, thus condition (35) becomes

$$0 < A \leqslant \tfrac{1}{2}. \tag{37}$$

Since $|A| \geqslant |B|$, relation (36) is automatically satisfied whenever (35) is.

For all

$$r > \frac{1}{4} - \frac{1}{P^2}$$

the denominator of A is positive, and (37) is then satisfied if and only if

$$(r - \tfrac{1}{2})(4 - P^2) \leqslant 0. \tag{38}$$

Thus for $|P| \leqslant 2$, (38) implies $0 < r \leqslant \frac{1}{2}$, and for $|P| > 2$, (38) implies $r > \frac{1}{2}$.

Thus the stable region predicted by linearization is the union of

$$[\mathrm{I}] \quad \{|\alpha h\bar{U}| \leqslant 2\} \cap \{r \leqslant \tfrac{1}{2}\}$$

and

$$[\mathrm{II}] \quad \{|\alpha h\bar{U}| \geqslant 2\} \cap \{r \geqslant \tfrac{1}{2}\}.$$

The exact stability condition for (15), given by (26) and (31), is

$$[\mathrm{III}] \quad \{|\alpha h U_{\max}| < 2\} \cap \{r < \tfrac{1}{2}\}.$$

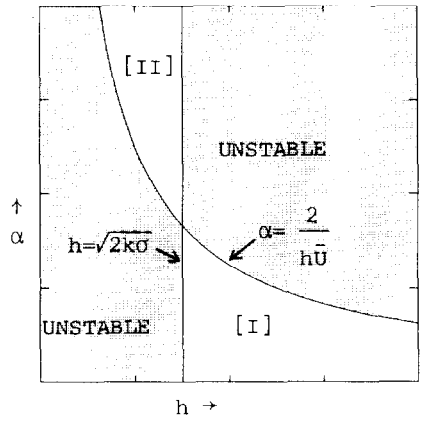

FIG. 1. Linearized stability region.

Figure 1 shows the stability regions in the αh-plane predicted to be stable by linearization for fixed k, σ, and $\bar{U} > 0$. Figure 2 shows the same for the exact stabilty condition, for fixed k, σ, and $U_{\max}$.

If the constant, $\bar{U}$ about which the perturbation is done, is taken to be $U_{\max}$ (see, for example, [6]), then regions [I] and [III] are the same. However, by allowing condition [II] also for stability, linearizing seriously misses the point. In the next section we shall demonstrate that condition [II] *is* however, valid for small perturbations about a constant, but is *not* valid for general initial conditions deviating far away from a constant solution.

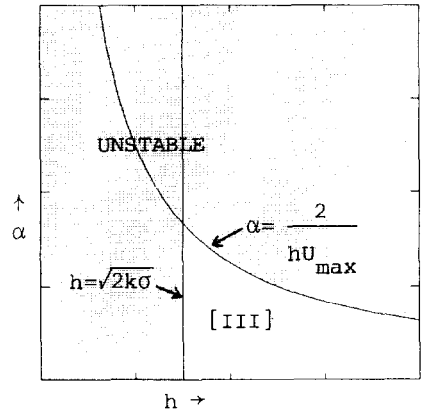

FIG. 2. Exact stability region.

6. Numerical Experiments

An Experiment with the Skew Scheme

The fact that the exact stability condition for the skew scheme, (17), imposes no restriction on positive α for positive initial conditions, as long as the linear stability condition (26) is satisfied, is remarkable. This implies that steep fronts will not become unstable even for very large nonlinear convection and very small diffusion. In the first experiment, we solve this scheme with periodic boundary conditions and the following initial condition:

$$u(x,0)=\begin{cases}0, & x\in[0,6]\\ 0.8\sin\left(\frac{\pi}{2}(x-6)\right), & x\in[6,7]\\ 0.8, & x\in[7,8]\\ 0.8\cos\left(\frac{\pi}{2}(x-8)\right), & x\in[8,9]\\ 0, & x\in[9,10].\end{cases} \tag{39}$$

The following parameters were used:

$$N=50,\qquad h=0.2,\qquad k=0.5,$$
$$\sigma=0.001,\qquad \alpha=1000.$$

Hence $r=0.0125<\frac{1}{2}$ and the linear stability condition is satisfied. With these parameters, we are solving the following equation numerically: $u_t=2uu_x+0.001u_{xx}$. Figure 3 shows the solution, printed every timestep for 38 timesteps.

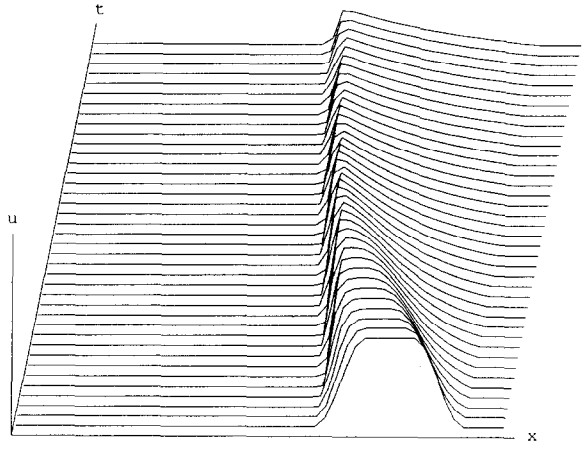

FIG. 3. Numerical solution of (17) with initial condition (39); $h=0.2$, $k=0.5$, $\sigma=0.001$, $\alpha=1000$.

Experiments with the Central Scheme

In the next three experiments, we solve the central scheme, (15), and show that the scheme is stable when both the linear (26) and the nonlinear conditions (31) are satisfied, and we also show the effects of having just one satisfied and the other violated. The following parameters were used in all three experiments:

$$N = 50, \qquad h = 0.2, \qquad \sigma = 1.$$

Periodic boundary conditions were used and the initial condition was (39), thus U_j^0 is positive for all j and $U_{\max} = 0.8$.

Figure 4 shows 30 timesteps of the solution for the parameters

$$k = 0.018, \qquad \alpha = 12.49;$$

hence $r = 0.45 < \frac{1}{2}$ and $\alpha h U_{\max} = 1.9984 < 2$. The solution is perfectly stable and, although the shock which forms is relatively sharp, it never becomes sharper than that which the grid can resolve.

We now solve (15) with the linear condition violated. The following parameters were used:

$$k = 0.022, \qquad \alpha = 12.49;$$

hence $\alpha h U_{\max} = 1.9948 < 2$, but $r = 0.55 \not< \frac{1}{2}$. Figure 5 shows 25 timesteps of the solution. The growth of the highest mode is clearly visible.

We next solve (15) with the nonlinear stability condition violated. The following parameters were used:

$$k = 0.0195, \qquad \alpha = 12.505;$$

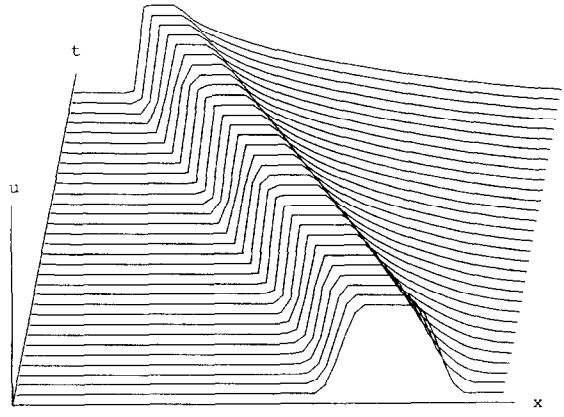

FIG. 4. Numerical solution of (15) with initial condition (39); $h = 0.2$, $k = 0.018$, $\sigma = 1$, $\alpha = 12.49$.

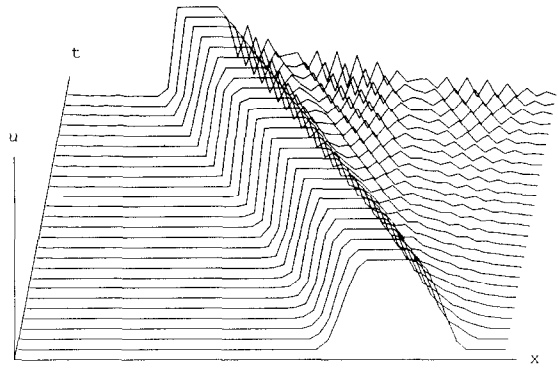

FIG. 5. Numerical solution of (15) with initial condition (39); $h = 0.2$, $k = 0.022$, $\sigma = 1$, $\alpha = 12.49$.

hence $r = 0.4875 < \frac{1}{2}$, but $\alpha h U_{\max} = 2.0008 \not< 2$. Figure 6 shows 25 timesteps of the solution. The pole-type of instability (a simple pole in time) is now clearly visible. Also note how the instability recovers after it has become negative.

The next three experiments demonstrate that the linearized stability analysis is valid for the ansatz for which it was derived, i.e., for a solution which is a small perturbation about a constant. The interesting point is that linearization predicts that for such solutions, the scheme is unstable when either of the exact linear or exact nonlinear stability condition is violated, *but that is stable when both are violated!* We shall use the following parameters in all three experiments:

$$N = 50, \qquad h = 0.2, \qquad \sigma = 1.$$

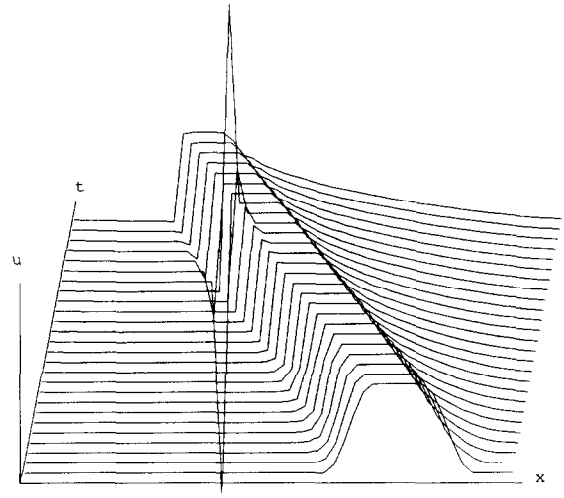

FIG. 6. Numerical solution of (15) with initial condition (39); $h = 0.2$, $k = 0.0195$, $\sigma = 1$, $\alpha = 12.505$.

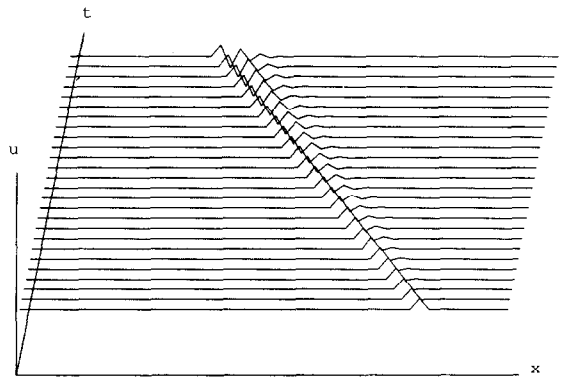

FIG. 7. Numerical solution of (15) with initial condition (40); $h = 0.2$, $k = 0.022$, $\sigma = 1$, $\alpha = 15.0$.

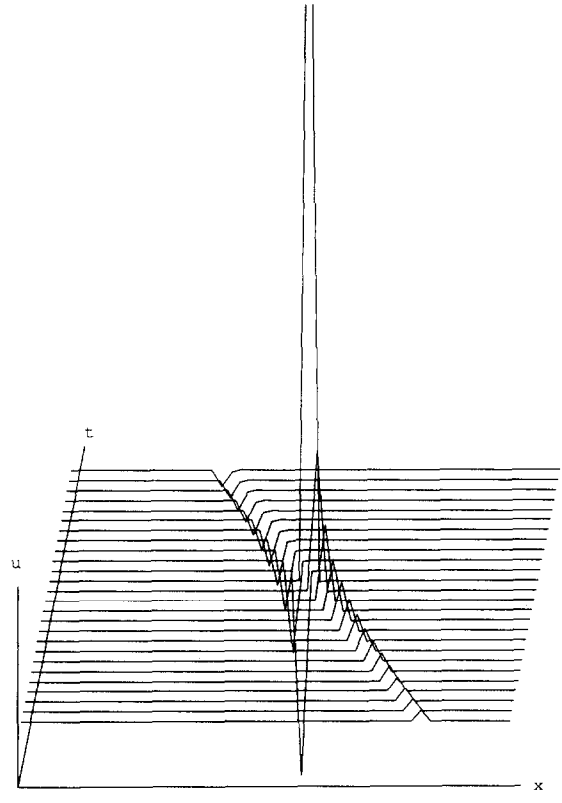

FIG. 8. Numerical solution of (15) with initial condition (40); $h = 0.2$, $k = 0.015$, $\sigma = 1$, $\alpha = 20.5$

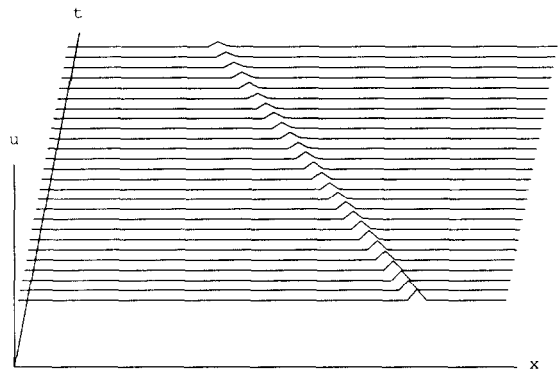

FIG. 9. Numerical solution of (15) with initial condition (40); $h = 0.2$, $k = 0.025$, $\sigma = 1$, $\alpha = 20.5$.

Figure 7 shows the solution of (15), with periodic boundary conditions and the following initial condition:

$$U_j^0 = \begin{cases} 0.5, & \text{for } j = 0, 1, ..., 39, 41, ..., 49, \\ 0.6, & \text{when } j = 40. \end{cases} \tag{40}$$

Thus $\bar{U} = 0.5$. The other parameters were

$$k = 0.022, \qquad \alpha = 15.0.$$

Here only the linear stability condition is violated: $r = 0.55$, but $\alpha h \bar{U} = 1.5$. The growth of a high wavenumber mode is clearly visible.

Figure 8 shows the solution of (15), with the same initial condition (40) and with the parameters:

$$k = 0.015, \qquad \alpha = 20.5.$$

Here only the nonlinear stability condition is violated: $\alpha h \bar{U} = 2.05$, but $r = 0.375$. The development of a nonlinear instability is witnessed.

Figure 9 shows the solution of (15), with the same initial condition (40) and with the parameters:

$$k = 0.025, \qquad \alpha = 20.5.$$

Here both stability conditions are violated: $\alpha h \bar{U} = 2.05$, and $r = 0.625$. No form of instability is seen. However, when the same parameters are used with an initial condition different from a perturbation about a constant solution, usually both types of instabilities are seen.

7. CONCLUSION

In this paper we have constructed a family of numerical schemes for Burgers' equation in the form of explicit partial difference equations on a uniform grid. The

solutions of these nonlinear difference equations can be related to the solutions of a discrete version of the linear heat equation by means of a family of discrete Hopf–Cole transformations. Since the dynamics of the linear equation is well understood, we can also analyse the dynamics of the nonlinear schemes and therefore establish conditions under which these schemes are guaranteed to be both linearly and nonlinearly stable.

We do not view these schemes so much as serious competitors for existing numerical methods to solve Burgers' equation, but rather as model equations which can develop a type of nonlinear instability which is not unlike that observed in many other existing schemes. In the present case, however, the actual mechanism by which the instabilities develop is fairly simple to analyse. We hope, therefore, that the results of our efforts will be useful to anyone wishing to gain more insight into the nature of nonlinear instabilities in numerical schemes.

In addition, we were also able to show, not only how well the results of a conventional linear stability analysis can predict the actual stability of one of our nonlinear schemes, but also in which respects such an analysis is misleading.

REFERENCES

1. L. N. TREFETHEN, *SIAM Rev.* **24**, 113 (1982).
2. L. N. TREFETHEN, *J. Comput. Phys.* **49**, 199 (1983).
3. L. N. TREFETHEN, *Commun. Pure Appl. Math.* **37**, 329 (1984).
4. M. B. GILES AND W. T. THOMPKINS, *J. Comput. Phys.* **58**, 349 (1985).
5. R. VICHNEVETSKY, *J. Numer. Methods Fluids* **9**, 623 (1989).
6. W. I. BRIGGS, A. C. NEWELL, AND T. SARIE, *J. Comput. Phys.* **51**, 83 (1983).
7. P.-Y. KUO AND J. M. SANZ–SERNA, *IMA J. Numer. Anal.* **1**, 215 (1981).
8. B. FORNBERG, *Math. Comput.* **27**, 45 (1973).
9. J. M. SANZ–SERNA, *SIAM J. Sci. Statist. Comput.* **6**, 923 (1985).
10. F. VADILLO AND J. M. SANZ–SERNA, *J. Comput. Phys.* **66**, 225 (1986).
11. J. M. SANZ–SERNA AND F. VADILLO, in *Numerical Analysis*, edited by D. F. Griffiths and G. A. Watson, Pitman Research Notes in Mathematics, Vol. 140 (Longman Scientific & Technical, New York, 1986).
12. I. S. GREIG AND J. LL. MORRIS, *J. Comput. Phys.* **20**, 64 (1976).
13. A. CLOOT AND B. M. HERBST, *J. Comput. Phys.* **75**, 31 (1988).
14. S. W. SCHOOMBIE, Numerical Analysis Report NA/109, University of Dundee, 1987 (unpublished).
15. D. M. SLOAN AND A. R. MITCHELL, *J. Comput. Phys.* **67**, 372 (1986).
16. D. M. SLOAN, *J. Comput. Phys.* **79**, 167 (1988).
17. E. HOPF, *Commun. Pure Appl. Math.* **3**, 201 (1950).
18. J. D. COLE, *Q. Appl. Math.* **9**, 225 (1951).
19. G. B. WHITHAM, *Linear and Nonlinear Waves* (Wiley, New York, 1974).
20. P. L. SACHDEV, *Z. Angew. Math. Phys.* **29**, 963 (1978).
21. H. TASSO AND J. TEICHMANN, *Z. Angew. Math. Phys.* **30**, 1023 (1979).
22. D. LEVI, O. RAGNISCO, AND M. BRUSCHI, *Nuovo Cimento* **74**, 33 (1983).
23. M. F. MARITZ, *Nuovo Cimento* **105**, 685 (1990).
24. M. R. SPIEGEL, *Finite Differences and Difference Equations* (McGraw–Hill, New York, 1971).
25. A. R. MITCHELL AND D. F. GRIFFITHS, *The Finite Difference Method in Partial Differential Equations* (Wiley, Chichester, 1980).